

Complexation of uranium(VI) with malonate at variable temperatures

By Linfeng Rao^{1,*}, Jun Jiang¹, PierLuigi Zanonato², Plinio Di Bernardo², Arturo Bismondo³ and Alexander Y. Garnov¹

¹ Glenn T. Seaborg Center, Lawrence Berkeley National Laboratory, Berkeley, CA 94720, USA

² Dipartimento di Chimica Inorganica Metallorganica ed Analitica, Università di Padova, via Loredan 4, I-35131 Padua, Italy

³ Istituto di Chimica e Tecnologie dei Materiali Avanzati del C.N.R. of Padova, Italy

(Received August 20, 2001; accepted April 11, 2002)

*Uranium(VI) / Malonate / Complexation /
Temperature effect / Stability constants / Enthalpy / Entropy*

Summary. The complexation between uranium(VI) and malonate in 1.05 mol kg⁻¹ NaClO₄ was studied at variable temperatures (25, 35, 45, 55 and 70 °C). The formation constants of three successive complexes, UO₂(OOCCH₂COO), UO₂(OOCCH₂COO)₂²⁻ and UO₂(OOCCH₂COO)₃⁴⁻, and the molar enthalpies of complexation were determined by potentiometry and calorimetry. The heat capacity of the complexation, $\Delta C_{p,m}^{\circ}(\text{ML}_j)$, is calculated to be 96 ± 12 , 195 ± 15 and $267 \pm 22 \text{ J K}^{-1} \text{ mol}^{-1}$ for $j = 1, 2$ and 3 , respectively. Extended X-ray Absorption Fine Structure Spectroscopy helped to characterize the coordination modes in the complexes in solution. UV/Vis absorption and luminescence spectra at different temperatures provided qualitative information on the temperature effect. The effect of temperature on the complexation between uranium(VI) and malonate is discussed in terms of the electrostatic model and compared with the complexation between uranium(VI) and acetate.

Introduction

Significant interest has been stimulated by the recent activities of the environmental management of nuclear wastes in the coordination chemistry of actinides in solution, especially at elevated temperatures. It is estimated that the temperature of the waste forms in the repository could vary from 100 to 300 °C [1], while the temperature in the waste storage tanks ranges from ambient to over 90 °C [2]. Consequently, accurate data on the chemical behavior of actinides at elevated temperatures are needed to develop the technologies for waste processing and disposal.

The majority of the available data on the complexation of actinides are for 25 °C [3]. Though data at other temperatures could be estimated by extrapolation assuming a constant enthalpy of complexation [4], such practice could lead to large uncertainties [5]. More recent theoretical models, such as the HKF equation of state [6–8], have been used to predict the thermodynamic properties of aqueous species under geothermal conditions. However, application of these

models to actinides is rare because the model parameters for actinides currently do not exist. As a result, reliable experimental data on the complexation of actinides in solution at elevated temperatures are still needed.

To provide such data, we have started investigations on the complexation of actinides and lanthanides with carboxylic acids at variable temperatures. The effect of temperature on the complexation of neodymium(III) [5] and uranium(VI) [9] with acetate has been studied and discussed in terms of a Born-type electrostatic model [10]. Results indicate that the complexation with acetate is entropy driven and enhanced at elevated temperatures. The enhancement was interpreted on the basis of the perturbation in the dielectric properties and the structure of the solvent – both in the primary hydration sphere and in the bulk. This paper summarizes the results of the complexation of uranium(VI) with malonate. This system has been previously studied at 25 °C [3, 11], but not at elevated temperatures. In the present work, thermodynamic parameters were determined by potentiometry and calorimetry. Spectroscopic techniques, including Extended X-ray Absorption Fine Structure (EXAFS), UV/Vis absorption and luminescence, were used in conjunction with the thermodynamic data to establish the coordination modes in the complexes. These data, while supporting the safe management of nuclear wastes, provide insight into the fundamental aspects of the coordination of actinides, such as the effect of temperature on the structure and dielectric property of the solvent, the solvation of both the metal and the ligand, and the energetics of the complexation [12–14].

Experimental

Chemicals

All chemicals were reagent grade or higher. Distilled water was used in preparations of all the solutions. Sodium hydroxide solutions, free from carbonate, were standardized against 1.005 mol dm⁻³ hydrochloric acid (Aldrich, ACS volumetric standard). The standardized sodium hydroxide solution was in turn used to determine the concentrations of perchloric acid and malonic acid by potentiometry. Buffer solutions of sodium malonate/malonic acid were prepared

* Author for correspondence (E-mail: LRao@lbl.gov).

by adding calculated amounts of perchloric acid into solutions of sodium malonate. The stock solution of uranyl perchlorate was prepared by dissolving uranium trioxide (UO_3) in perchloric acid (Aldrich, 70%). The concentrations of uranium and perchloric acid in the stock solution were determined by EDTA titration complexometry [15] and fluorimetry [16], and Gran's potentiometric method [17], respectively. The ionic strength of all the solutions used in potentiometry and calorimetry was adjusted to 1.0 mol dm^{-3} at 25°C by adding appropriate amounts of sodium perchlorate.

Potentiometry

Potentiometric experiments were carried out at 25, 35, 45, 55, and 70°C with a variable-temperature titration setup. Detailed description of the apparatus and the procedures have been previously provided [5, 9, 18]. The protonation of malonate was studied by titrating a buffered malonate solution (0.06 mol dm^{-3}) with HClO_4 or a malonic acid solution (0.06 mol dm^{-3}) with NaOH . The complexation between uranium(VI) and malonate was studied by titrating a solution of uranyl perchlorate ($0.006\text{--}0.015 \text{ mol dm}^{-3}$) with a buffered malonate solution. Multiple titrations were conducted at each temperature with different concentrations of uranyl perchlorate. The initial volume of the test solutions ranged from 40 to 95 cm^3 at 25°C . The computer program Superquad [19] was used to calculate the protonation constants of malonate, $\beta_{j,H}$, and the formation constants of uranyl malonate complexes, $\beta_{j,M}$, on the molarity scale.

To compare the results at different temperatures, the constants calculated on the molarity scale were converted to the values on the molality scale, using $\beta_{j,m} = \beta_{j,M} \times (d_{298})^j$ [20], where d_{298} ($= 1.073 \text{ g cm}^{-3}$) is the density of 1.0 mol dm^{-3} sodium perchlorate in water at 25°C [21]. This solution, equivalent to 1.05 mol kg^{-1} sodium perchlorate, is chosen as the reference solution for the calculation of the stability constants on the molality scale.

Calorimetry

Calorimetric titrations were conducted with a computer-controlled isoperibol calorimeter (Model ISC-4285, Calorimetry Sciences Corp.). Detailed description of the instrument was provided elsewhere [9]. The performance of the calorimeter was previously tested by measuring the enthalpy of protonation of 2-bis(2-hydroxyethyl)amino-2-hydroxymethylpropan-1,3-diol at different temperatures ($25\text{--}80^\circ\text{C}$) [9, 22]. The concentrations of the cup solutions and the titrants in the calorimetric titrations were similar to those in the potentiometric titrations, except that the initial volume of the cup solution was 20 cm^3 at 25°C . The enthalpy of malonate protonation and complexation with uranium(VI) were calculated with the computer program Letagrop [23] as previously described.

Extended X-ray absorption fine structure (EXAFS) spectroscopy

EXAFS experiments were conducted with three uranyl solutions (I to III). Solution I ($\text{pH} \sim 1$) contains 20 mmol dm^{-3} uranyl perchlorate and 100 mmol dm^{-3} perchloric acid so

the uranyl species is $\text{UO}_2^{2+}(\text{aq})$. Solution II ($\text{pH} = 3.5$) contains 13 mmol dm^{-3} uranyl perchlorate, 38 mmol dm^{-3} malonic acid and 71 mmol dm^{-3} sodium malonate. Solution III contains 5.5 mmol dm^{-3} uranyl perchlorate, 5.5 mmol dm^{-3} malonic acid and appropriate amounts of NaOH to achieve a pH of 5.2. Speciation calculations with the formation constants [9, 11] show that the dominant uranyl species in Solutions II and III are 1 : 2 and 1 : 1 uranyl malonate complexes, respectively. Approximately 2 cm^3 of the solution was sealed in a polyethylene tube (5 mm i.d.) and mounted on an aluminum sample positioner with Scotch tape for the EXAFS experiments.

Uranium L_3 -edge EXAFS spectra were collected at the Stanford Synchrotron Radiation Laboratory (SSRL) on wiggler beamline 4-1 under normal ring operating conditions (3.0 GeV , $50\text{--}100 \text{ mA}$). The EXAFS data were collected in both the transmission (using argon-filled ionization chambers) and the fluorescence modes (using a four-element Ge-detector [24]), up to $k \sim 15 \text{ \AA}^{-1}$. Eight scans were performed for each sample. Energy calibration was based on assigning the first inflection point of the absorption edge for uranium dioxide (UO_2) to 17166 eV . The EXAFS spectra were fitted with the *R*-space X-ray Absorption Package (RSXAP) [25], using parameterized phase and amplitude functions generated by the program FEFF8 [26] with the reference crystal structure of $\text{Ba}[\text{UO}_2(\text{OOCCH}_2\text{COO})_2] \cdot 3\text{H}_2\text{O}$ [27]. Standard scattering paths, including the single scattering $\text{U}\text{--}\text{O}_{\text{ax}}$ (axial oxygen), $\text{U}\text{--}\text{O}_{\text{eq}}$ (equatorial oxygen) and $\text{U}\text{--}\text{C}$, and the multiple scattering of $\text{O}=\text{U}=\text{O}$ (axial oxygens), were calculated from the reference structure and included in the data analysis. Full cluster multiple scattering calculations were tried but were found to have no effect on the best fit parameters or the overall goodness of the fit.

UV/Vis absorption and luminescence spectroscopy

UV/Vis absorption spectra were collected at 25 and 70°C on a Varian Cary-5G spectrometer equipped with a 1×1 Peltier automatic temperature controller. Ten mm quartz cells were used. Luminescence spectra were collected on a FluoroMax-2 spectrometer (Jobin Yvon-Spex Instruments S.A., Inc.) with 10 mm quartz fluorometer cells. The emission spectra of the uranyl solutions ($450\text{--}600 \text{ nm}$) were obtained from the excitation at 420 nm . A water-jacketed cuvette holder was used to maintain the sample solutions at the desired temperatures.

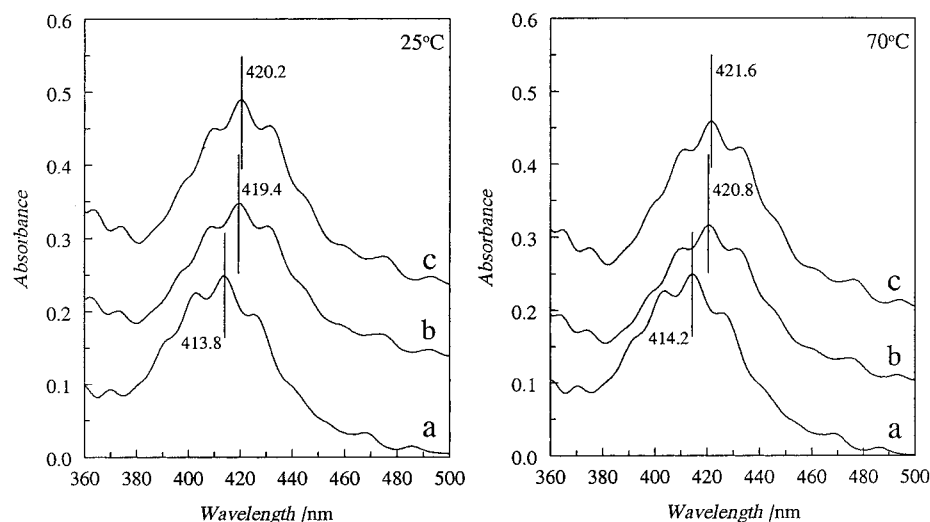
Results

Protonation of malonate

The calculated protonation constants, Gibbs free energy, enthalpy, and entropy of protonation are given in Table 1. The data for 25°C are in excellent agreement with the values in the literature [11]. As is typical of many carboxylic acids [3], the enthalpies of protonation of malonate are small (a few kJ mol^{-1}) and more endothermic at higher temperatures. Despite that the enthalpy becomes more unfavorable to the protonation at higher temperatures, the protonation constants increase slightly when the temperature is increased, largely due to the increasingly more positive entropy of protonation at higher temperatures (Table 1).

Table 1. Thermodynamic parameters of malonate protonation and complexation with the uranyl ion, $I = 1.05 \text{ mol kg}^{-1}$ (NaClO_4), the error limits represent 3σ . Data marked “*” are from Ref. [11].

| | T , °C | $\log \beta_{j,H}$ or $\log \beta_{j,M}$ | $\log \beta_{j,m}$ | $-\Delta G_{j,m}^{\circ}$ kJ mol^{-1} | $\Delta H_{j,m}^{\circ}$ kJ mol^{-1} | $\Delta S_{j,m}^{\circ}$ $\text{J K}^{-1} \text{ mol}^{-1}$ |
|--|-------------|---|--------------------|---|--|--|
| $\text{H}^+ + \text{L}^{2-} = \text{HL}^-$ | 25 | 5.10 ± 0.01 $5.09 \pm 0.02^*$ | 5.14 ± 0.01 | 29.3 ± 0.1 | 2.07 ± 0.03 2.0^* | 105 ± 1 105^* |
| | 35 | 5.15 ± 0.01 | 5.18 ± 0.01 | 30.6 ± 0.1 | 3.12 ± 0.03 | 109 ± 1 |
| | 45 | 5.17 ± 0.01 | 5.20 ± 0.01 | 31.7 ± 0.1 | 4.34 ± 0.03 | 113 ± 1 |
| | 55 | 5.22 ± 0.01 | 5.25 ± 0.01 | 33.0 ± 0.1 | 5.55 ± 0.04 | 117 ± 1 |
| | 70 | 5.29 ± 0.02 | 5.32 ± 0.02 | 35.0 ± 0.1 | 7.08 ± 0.08 | 122 ± 1 |
| $2\text{H}^+ + \text{L}^{2-} = \text{H}_2\text{L}$ | 25 | 7.69 ± 0.01 $7.68 \pm 0.03^*$ | 7.75 ± 0.01 | 44.2 ± 0.1 | 0.43 ± 0.03 0.5^* | 150 ± 1 150^* |
| | 35 | 7.82 ± 0.01 | 7.88 ± 0.01 | 46.5 ± 0.1 | 2.58 ± 0.03 | 159 ± 1 |
| | 45 | 7.83 ± 0.02 | 7.89 ± 0.02 | 48.1 ± 0.1 | 4.72 ± 0.03 | 166 ± 1 |
| | 55 | 7.91 ± 0.02 | 7.97 ± 0.02 | 50.1 ± 0.1 | 6.84 ± 0.03 | 173 ± 1 |
| | 70 | 8.00 ± 0.02 | 8.06 ± 0.02 | 52.9 ± 0.1 | 10.06 ± 0.08 | 184 ± 1 |
| $\text{UO}_2^{2+} + \text{L}^{2-} = \text{UO}_2\text{L}$ | 25 | 5.36 ± 0.01 $5.42 \pm 0.2^*$ | 5.39 ± 0.01 | 30.8 ± 0.1 | 8.0 ± 0.7 8.7^* | 130 ± 2 134^* |
| | 35 | 5.42 ± 0.01 | 5.45 ± 0.01 | 32.2 ± 0.1 | 9.8 ± 0.3 | 136 ± 1 |
| | 45 | 5.56 ± 0.01 | 5.59 ± 0.01 | 34.0 ± 0.1 | 10.7 ± 0.2 | 141 ± 1 |
| | 55 | 5.67 ± 0.01 | 5.70 ± 0.01 | 35.8 ± 0.1 | 11.5 ± 0.2 | 144 ± 1 |
| | 70 | 5.80 ± 0.01 | 5.83 ± 0.01 | 38.3 ± 0.1 | 12.5 ± 0.4 | 148 ± 1 |
| $\text{UO}_2^{2+} + 2\text{L}^{2-} = \text{UO}_2\text{L}_2^{2-}$ | 25 | 9.39 ± 0.01 $9.48 \pm 0.2^*$ | 9.45 ± 0.01 | 53.9 ± 0.1 | 11 ± 1 11^* | 218 ± 4 220^* |
| | 35 | 9.74 ± 0.02 | 9.80 ± 0.02 | 57.8 ± 0.1 | 13.4 ± 0.4 | 231 ± 2 |
| | 45 | 9.85 ± 0.02 | 9.91 ± 0.02 | 60.4 ± 0.1 | 16.0 ± 0.4 | 240 ± 2 |
| | 55 | 10.05 ± 0.02 | 10.11 ± 0.02 | 63.5 ± 0.1 | 17.4 ± 0.4 | 246 ± 2 |
| | 70 | 10.35 ± 0.01 | 10.41 ± 0.01 | 68.4 ± 0.1 | 19.8 ± 0.5 | 257 ± 2 |
| $\text{UO}_2^{2+} + 3\text{L}^{2-} = \text{UO}_2\text{L}_3^{4-}$ | 25 | 11.22 ± 0.06 | 11.31 ± 0.06 | 64.6 ± 0.3 | 11.7 ± 4.0 | 256 ± 14 |
| | 35 | 12.43 ± 0.06 | 12.52 ± 0.06 | 73.8 ± 0.4 | 15.6 ± 0.7 | 290 ± 3 |
| | 45 | 12.72 ± 0.08 | 12.81 ± 0.08 | 78.0 ± 0.5 | 18.7 ± 0.6 | 304 ± 3 |
| | 55 | 13.16 ± 0.12 | 13.25 ± 0.12 | 83.2 ± 0.8 | 20.4 ± 0.6 | 316 ± 4 |
| | 70 | 13.61 ± 0.02 | 13.70 ± 0.02 | 90.0 ± 0.1 | 24.1 ± 0.8 | 332 ± 3 |

**Fig. 1.** Absorption spectra of uranyl malonate solutions at 25 and 70 °C. (a) $200 \text{ mmol dm}^{-3} \text{UO}_2(\text{ClO}_4)_2/600 \text{ mmol dm}^{-3} \text{HClO}_4$. (b) $10 \text{ mmol dm}^{-3} \text{UO}_2(\text{ClO}_4)_2/50 \text{ mmol dm}^{-3}$ malonic acid (pH 3). (c) $10 \text{ mmol dm}^{-3} \text{UO}_2(\text{ClO}_4)_2/100 \text{ mmol dm}^{-3}$ malonic acid (pH 3).

UV/Vis absorption and luminescence spectra of uranyl malonate

Fig. 1 shows the absorption spectra of the three uranyl solutions at 25 and 70 °C. The ratios of $C_{\text{malonate}}/C_{\text{U}}$ are 0, 5 and 10, respectively. The vibronic structure due to the

symmetric stretching vibration of the dioxo cation [28, 29] is quite similar at 25 and 70 °C. At each temperature, the spectra were red-shifted as $C_{\text{malonate}}/C_{\text{U}}$ was increased. The shifts at 70 °C ($\Delta\lambda_{a-b} = 6.6 \text{ nm}$, $\Delta\lambda_{a-c} = 7.4 \text{ nm}$) are slightly larger than those at 25 °C ($\Delta\lambda_{a-b} = 5.6 \text{ nm}$, $\Delta\lambda_{a-c} = 6.4 \text{ nm}$).

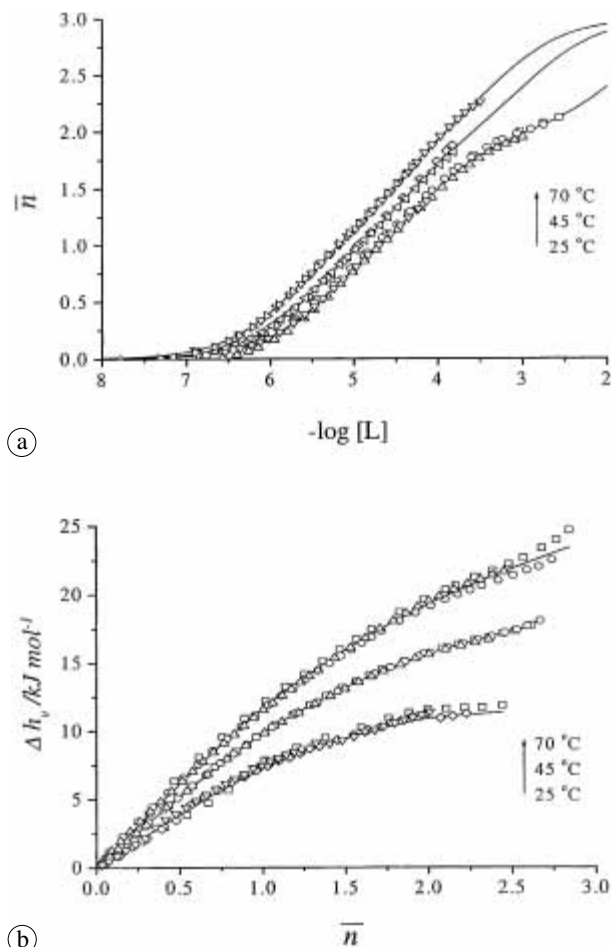


Fig. 2. Potentiometric and calorimetric titrations of the uranyl malonate system. $I = 1.05 \text{ mol kg}^{-1} \text{ NaClO}_4$. Titrant: $498 \text{ mmol dm}^{-3} \text{ CH}_2(\text{COONa})_2 + 348 \text{ mmol dm}^{-3} \text{ HClO}_4$. 50–70 data points were collected in each titration (the number of points in the figure is reduced for clarity). (a) Potentiometry: The complex formation function (\bar{n}) as a function of $\log[\text{L}]$. Initial cup solutions ($\text{UO}_2(\text{ClO}_4)_2/\text{HClO}_4$ in mmol dm^{-3}): (\square) 40 mL, 5.57/5.96; (\circ) 40 mL, 9.46/10.13; (\triangle) 40 mL, 13.92/14.90; (∇) 95 mL, 5.00/5.00; (\diamond) 80 mL, 5.00/5.00; (\leftarrow) 80 mL, 12.00/12.00; (\rightarrow) 95 mL, 12.00/12.00. (b) Calorimetry: Total heat per mole of uranium as a function of \bar{n} . Initial cup solutions (20 mL $\text{UO}_2(\text{ClO}_4)_2/\text{HClO}_4$ in mmol dm^{-3}): (\square) 5.87/5.98; (\diamond) 9.46/10.13; (∇) 13.92/14.90; (\circ) 9.98/10.17; (\triangle) 14.67/14.95.

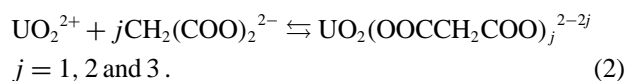
No significant shifts in the positions of the luminescence emission bands (480–580 nm) were observed when the temperature of the uranyl malonate solutions was increased from 25 to 70 °C. However, the overall intensities of the bands decreased by about ten times at 70 °C, compared to those at 25 °C. In addition, the relative intensities of the individual bands changed significantly when the temperature was increased.

Thermodynamic parameters for the complexation of uranium(VI) with malonate

The potentiometric titration data for the complexation of uranium(VI) with malonate are presented in Fig. 2a, in the form of \bar{n} vs. $\log[\text{L}]$. \bar{n} is the average number of malonate ions bound to each uranyl ion as calculated by the equation:

$$\bar{n} = \left\{ C_L - [\text{L}] \left(1 + \beta_{1,\text{H}}[\text{H}^+] + \beta_{2,\text{H}}[\text{H}^+]^2 \right) \right\} / C_M \quad (1)$$

C_L and C_M are the concentrations of total malonate and uranium(VI) in solution and $[\text{L}]$ is the concentration of free malonate. $\beta_{1,\text{H}}$ and $\beta_{2,\text{H}}$ are the overall protonation constants obtained from the protonation titration: $\beta_{1,\text{H}} = [\text{HL}^-]/([\text{H}^+][\text{L}^-])$ and $\beta_{2,\text{H}} = [\text{H}_2\text{L}]/([\text{H}^+]^2[\text{L}^-])$. Data analysis by the Superquad program indicates that the best fit was obtained by assuming the formation of three complexes:



The calculated formation constants and Gibbs free energy of complexation are given in Table 1. Including the third complex in the fit improves the overall fit, but has minor effect on the constants for the first and the second complexes. The highest value of \bar{n} in the experiments was 2.26 and the maximum percentage of the third complex was about 35%. Using these constants, simulated potentiometric titration curves are calculated and found in good agreement with the experimental points (Fig. 2a). The data in Table 1 indicate that the complexation between uranium(VI) and malonate is enhanced by elevated temperatures. The 1 : 1 and 1 : 2 complexes at 70 °C are about 2.8 and 9.1 times stronger than those at 25 °C.

The data of the calorimetric titrations are shown in Fig. 2b, in the form of Δh_v vs. \bar{n} , where Δh_v is the total heat per mole of uranium and calculated by dividing the net reaction heat with the number of moles of uranium in the calorimeter vessel. The enthalpy changes of the complexation are summarized in Table 1. The molar enthalpy of complexation increases monotonously as the temperature is increased. Again, simulated calorimetric titration curves were calculated with the values of $\log \beta$ and ΔH° of complexation and protonation constants and enthalpies in Table 1 and found consistent with the experimental data (Fig. 2b).

Coordination modes in the uranyl malonate complexes

Fig. 4 shows the background subtracted EXAFS spectra and the corresponding Fourier transforms for three uranyl malonate solutions, as well as the results for the uranyl acetate complexes from the literature [9] for comparison. The best fit parameters are given in Table 2.

The EXAFS data analysis yields two axial oxygens at a distance of 1.77–1.79 Å for all the three uranyl malonate solutions, and five to six equatorial oxygens at distances of 2.34–2.41 Å. Solution I does not contain malonate and the only uranyl species is the free $\text{UO}_2^{2+}(\text{aq})$ ion. The best fit indicates that there are 5.5 oxygens (from water molecules) in the equatorial plane at a distance of 2.41 Å. For Solution II, which contains dominantly the 1 : 2 uranyl malonate complex by speciation calculation based on the formation constants in Table 1, the EXAFS data were fitted with either one or two equatorial oxygen shells. The one- O_{eq} -shell model yields 5.7 equatorial oxygens at 2.37 Å, while the two- O_{eq} -shell model yields 4 oxygens at 2.34 Å and 2 oxygens at 2.40 Å (Table 2). Though either of the two models seems to provide fairly good fit to the experimental spectra, the overall goodness of the fit by the two-shell model is

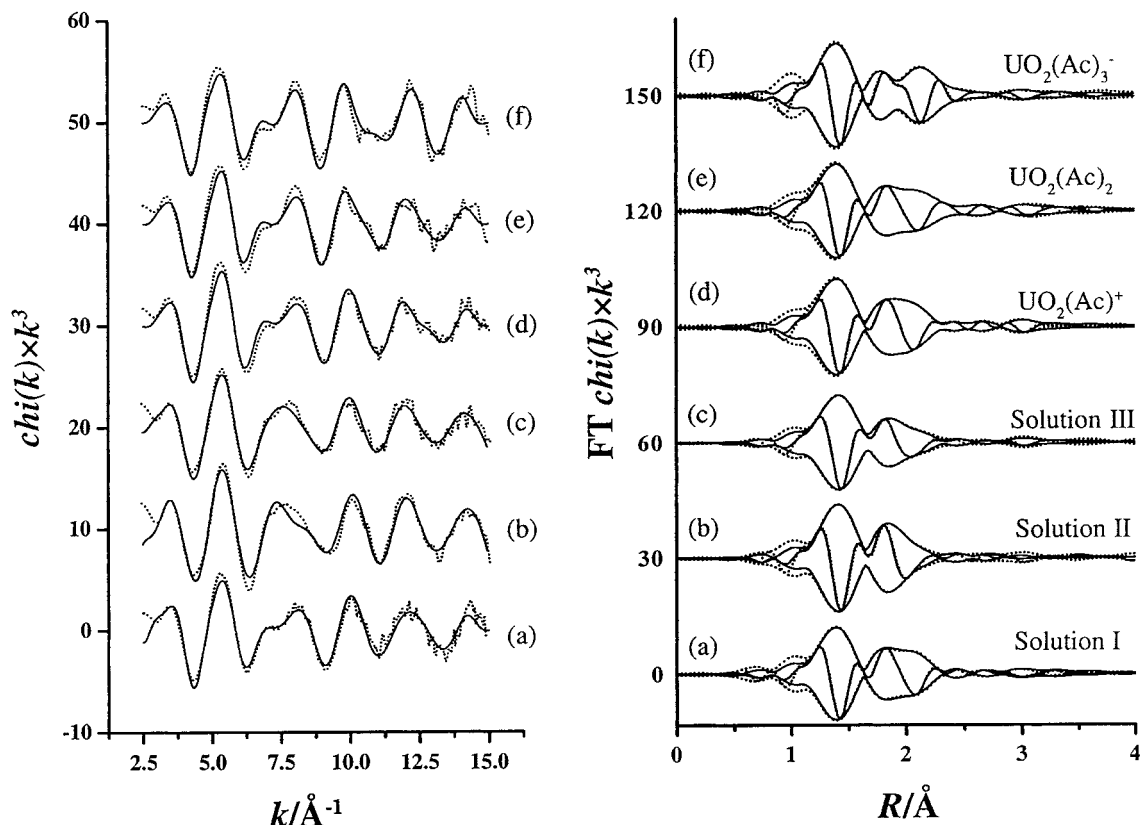


Fig. 3. Experimental (dotted lines) and fitted (solid lines) uranium L_3 -edge EXAFS spectra (A) and associated Fourier Transforms (B). (a) Solution I, (b) Solution II, (c) Solution III, (d) $\text{UO}_2(\text{OOCCH}_3)^+$ (aq) [9], (e) $\text{UO}_2(\text{OOCCH}_3)_2$ (aq) [9], (f) $\text{UO}_2(\text{OOCCH}_3)_3^-$ (aq) [9].

Table 2. Fitting parameters for U L_3 -edge EXAFS (the data for uranyl acetate complexes are from the literature [9]).

| Samples | Shell | R^a , Å | N^a | σ^b Å | ΔE_0 , eV | |
|---|--------------------------------------|--------------------|-------|--------------|-------------------|--------|
| Solution I Uranyl perchlorate (0.1 M perchloric acid) | U–O _{ax} | 1.77 | 1.8 | 0.0385 | –13.69 | |
| | U–O _{eq} | 2.41 | 5.5 | 0.0871 | –13.69 | |
| Solution II 1 : 2 uranyl/malonate (pH = 3.5) | Two | U–O _{ax} | 1.78 | 2.0 | 0.0342 | –12.77 |
| | O _{eq} -shell | U–O _{eq1} | 2.34 | 3.9 | 0.0815 | –12.77 |
| | model | U–O _{eq2} | 2.40 | 1.9 | 0.0790 | –12.77 |
| Solution III 1 : 1 uranyl/malonate (pH = 5.2) | One | U–O _{ax} | 1.77 | 2.0 | 0.0405 | –12.84 |
| | O _{eq} -shell model | U–O _{eq} | 2.37 | 5.7 | 0.0902 | –12.84 |
| Solution III 1 : 1 uranyl/malonate (pH = 5.2) | U–O _{ax} | 1.79 | 2.3 | 0.0501 | –14.01 | |
| | U–O _{eq} | 2.39 | 5.2 | 0.0995 | –14.01 | |
| | $\text{UO}_2(\text{OOCCH}_3)^+$ (aq) | U–O _{ax} | 1.78 | 2.0 | 0.0411 | –14.48 |
| | | U–O _{eq1} | 2.38 | 4.0 | 0.0703 | –14.48 |
| U–O _{eq2} | | 2.50 | 2.0 | 0.0920 | –14.48 | |
| U–C | | 2.91 | 1.3 | 0.0500 | –14.48 | |
| $\text{UO}_2(\text{OOCCH}_3)_2$ (aq) | U–O _{ax} | 1.78 | 2.0 | 0.0370 | –12.45 | |
| | U–O _{eq} | 2.42 | 5.9 | 0.0888 | –12.45 | |
| | U–C | 2.90 | 2.2 | 0.0500 | –12.45 | |
| $\text{UO}_2(\text{OOCCH}_3)_3^-$ (aq) | U–O _{ax} | 1.78 | 2.0 | 0.0344 | –12.37 | |
| | U–O _{eq1} | 2.34 | 1.9 | 0.0533 | –12.37 | |
| | U–O _{eq2} | 2.48 | 4.1 | 0.0482 | –12.37 | |
| | U–C | 2.87 | 2.1 | 0.0500 | –12.37 | |

a: The 95% confidence limits for the bond lengths (R) and coordination numbers (N) for each shell are: U–O_{ax}, 0.01 Å and $\pm 15\%$; U–O_{eq}, 0.02 Å and $\pm 25\%$; U–C, 0.02 Å and $\pm 25\%$, respectively;

b: σ is the EXAFS Debye–Waller term which accounts for the effects of thermal and static disorder through damping of the EXAFS oscillations by the factor $\exp(-2k^2\sigma^2)$.

better. The value of R (%) (a measure of the overall goodness of the fit in the RSXAP package [25]) was 3.19 and 2.21 for the one and two-shell models, respectively. For Solution III, the EXAFS analysis yields 5 equatorial oxygens at 2.39 Å.

Discussion

Effect of temperature on the complexation

While the UV absorption (Fig. 1) and luminescence spectra qualitatively demonstrate that the increase in the temperature affects the complexation, the effect is quantified by the thermodynamic data in Table 1. Though the potentiometric titration data yield the constants for three uranyl malonate complexes, the uncertainty in the constant for the third complex is higher than the first two because it was never dominant under the experimental conditions (< 35%). As a result, the following discussions are mostly focused on the 1 : 1 and 1 : 2 complexes.

The formation constants of the 1 : 1 and 1 : 2 complexes increase by 2.8 and 9.1 times, respectively, as the temperature is increased from 25 °C to 70 °C. Similar effects of temperature were previously observed for a few other complexation systems [5, 9, 30, 31]. For example, the formation constant of the 1 : 1 neodymium(III) acetate, $\text{Nd}(\text{OOCCH}_3)_2^{2+}$, increases from 96 ± 9 (25 °C) to 200 ± 4 (70 °C), a 2-fold increase [5]. The formation constant of the 1 : 1 uranyl acetate, $\text{UO}_2(\text{OOCCH}_3)^+$, increases from 407 ± 27 (25 °C) to 1020 ± 110 (70 °C), a 2.5-fold increase [9]. These observations have been interpreted by the Born-type electrostatic model [5, 9] where the temperature effect is expressed as

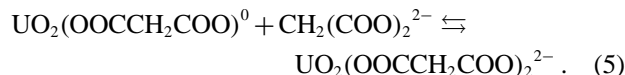
$$\frac{\partial(\log \beta)}{\partial T} = N e^2 Z_1 Z_2 / (0.2303 R d_{12}) \times (1/T - 1/219) / (\varepsilon T), \quad (3)$$

where ε is the dielectric constant of water and a function of temperature [32, 33]. Z_1 and Z_2 are the charges of the two species. Other parameters in Eq. (3) are explained elsewhere [34, 35].

Since T is always higher than 219 K in the whole accessible temperature range for liquid water, the electrostatic model predicts $\partial(\log \beta)/\partial T > 0$ if $Z_1 Z_2 < 0$. In other words, the complexation between species of opposite charges is strengthened by the increase in temperature. This is consistent with the experimental results for the 1:1 complexes of neodymium(III) acetate [5], uranyl acetate [9], and uranyl malonate. In addition, the electrostatic model predicts that the magnitude of the temperature coefficient, $\partial(\log \beta)/\partial T$, is proportional to $|Z_1 Z_2|$. In other words, the complexation between species with higher charges is more sensitive to the change in temperature. The data in Table 3 on three

1 : 1 complexes seem to support this prediction. However, more studies of diversified complexation systems covering a wider range of $|Z_1 Z_2|$ are needed to allow further tests of the prediction.

The electrostatic model predicts that the complexation with a neutral species should be insensitive to the change in temperature ($|Z_1 Z_2| = 0$, then $\partial(\log \beta)/\partial T = 0$). The stepwise formation of the 1 : 3 uranyl acetate complex and 1 : 2 uranyl malonate complex belongs to this category:



The data on reaction 4 indicate that, indeed, the formation constant of reaction 4 remains unchanged in the temperature range from 25 to 70 °C [9]. However, the data from this work indicate that there is a 3-fold increase in the formation constant of reaction 5 when the temperature is increased from 25 to 70 °C. This disagreement may reflect that electrostatic interactions should not be completely ignored in the complexation involving a neutral species due to the charge distribution and/or inductive effect. Besides, other factors in addition to electrostatic interactions may play important roles in the energetics of the complexation. More detailed and quantitative discussions on this subject will become feasible when a wider range of complex systems are studied at variable temperatures.

Data in Table 1 show that, in the temperature range from 25 °C to 70 °C, both the enthalpy and entropy of complexation are positive. The complexation is entropy-driven, characteristic of the interaction between the “A-character” cations and anions [13]. As the temperature is increased, the entropy term ($T\Delta S_m^\circ$) increases more significantly than the enthalpy, resulting in even larger contributions from the entropy to the Gibbs free energy (ΔG_m°) and more stable complexes at higher temperatures. The increase of entropy with the temperature could be the consequence of a more disordered bulk water structure at higher temperatures due to the perturbation by thermal movements. In the process of complexation, the solvating water molecules are released to an already expanded and more disordered bulk solvent [12]. As a result, the net gain in the complexation entropy is larger at higher temperatures.

The molar enthalpy of complexation as a function of temperature can be fitted with linear equations, the slopes of which correspond to the heat capacity of the complexation, $\Delta C_{p,m}^\circ(\text{ML}_j)$. In the temperature range from 25 °C to 70 °C, values of $\Delta C_{p,m}^\circ$ for the 1 : 1, 1 : 2 and 1 : 3 uranyl malonate complexes are all positive and independent of temperature (96 ± 12 , 195 ± 15 and $267 \pm 22 \text{ J K}^{-1} \text{ mol}^{-1}$, respectively).

Table 3. Temperature effect on the formation constants of three 1 : 1 complexes.

| Reaction | $Z_1 Z_2$ | β_{70}/β_{25} | Reference |
|---|-------------------|-------------------------|-----------|
| $\text{Nd}^{3+} + \text{CH}_3\text{COO}^- \rightarrow \text{Nd}(\text{OOCCH}_3)_2^{2+}$ | -3 | 2 | [5] |
| $\text{UO}_2^{2+} + \text{CH}_3\text{COO}^- \rightarrow \text{UO}_2(\text{OOCCH}_3)^+$ | -3.2 ^a | 2.5 | [9] |
| $\text{UO}_2^{2+} + \text{CH}_2(\text{COO})_2^{2-} \rightarrow \text{UO}_2(\text{OOCCH}_2\text{COO})$ | -6.4 ^a | 2.8 | this work |

a: based on the effective charge on uranium(VI) [34, 35].

Coordination modes and thermodynamic trends

Coordination modes

The coordination of a carboxylate group to metal ions could take different modes, including unidentate [9, 36], bidentate [9, 37], bridging or “pseudobridging” [38]. The unidentate and bidentate modes of acetate have been identified in solution [9, 39] and shown to impact the thermodynamics of the complexation [9].

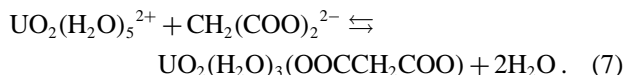
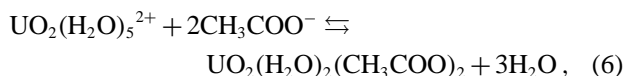
For the complexation of uranium(VI) with malonate, crystal structure data indicate that, while malonate “globally” forms bidentate complex with uranium(VI), each carboxylate group is unidentate with only one oxygen coordinating to the metal center [27, 40]. In this mode, the distance between the uranium and the malonate oxygens ranges from 2.32 to 2.36 Å. The best fit of the EXAFS spectra of Solution II (1 : 2 uranyl malonate complex) indicates that there are four oxygens at 2.34 Å and two oxygens at 2.40 Å (Table 2), consistent with two “globally” bidentate malonates and probably one or two water molecules in the equatorial plane. The EXAFS data on Solution III are not conclusive in defining the structure of the 1 : 1 complex, showing five equatorial oxygens at 2.39 Å. Probably this oxygen shell consists of one bidentate malonate and three water molecules and they are not distinguished by the EXAFS data.

It is interesting to compare the EXAFS results for uranyl malonate with those for uranyl acetate. Unlike malonate in which each carboxylate group can only be unidentate to the uranyl ion, acetate can coordinate to uranyl ion in bidentate ($R_{U-O} \sim 2.45\text{--}2.48$ Å) or unidentate ($R_{U-O} \sim 2.35$ Å) modes. EXAFS can differentiate the two modes by

the difference in R_{U-O} and the identification of the carbon atom in the bidentate mode ($R_{U-C} \sim 2.85\text{--}2.88$ Å) [9, 39]. As shown in Fig. 3, the Fourier Transforms for the solutions of uranyl acetate (curves d, e, f) show systematic changes in the region around 2 Å. These spectra have suggested one unidentate and two bidentate acetates in the third complex and helped to interpret the thermodynamic trends in the complexation of uranyl ion with acetate [9].

Comparison between the overall formation of $UO_2(OOCCH_3)_2$ and $UO_2(OOCCH_2COO)$

Both $UO_2(OOCCH_3)_2$ and $UO_2(OOCCH_2COO)$ involve two carboxylate groups but the latter is a chelate complex. Based on the EXAFS results in the literature [9] and the best fits for the EXAFS data in this work, the structures of the two complexes are suggested as shown in Fig. 4. The overall complexation reactions are postulated as



The thermodynamic parameters for reactions 6 and 7 are also compared in Fig. 4. The trends in the enthalpy and entropy are: 1) Both ΔH° and $T\Delta S^\circ$ for $UO_2(OOCCH_2COO)$ are smaller than those for $UO_2(OOCCH_3)_2$ at all temperatures; 2) ΔH° and $T\Delta S^\circ$ for $UO_2(OOCCH_2COO)$ are less sensitive to the temperature change than those

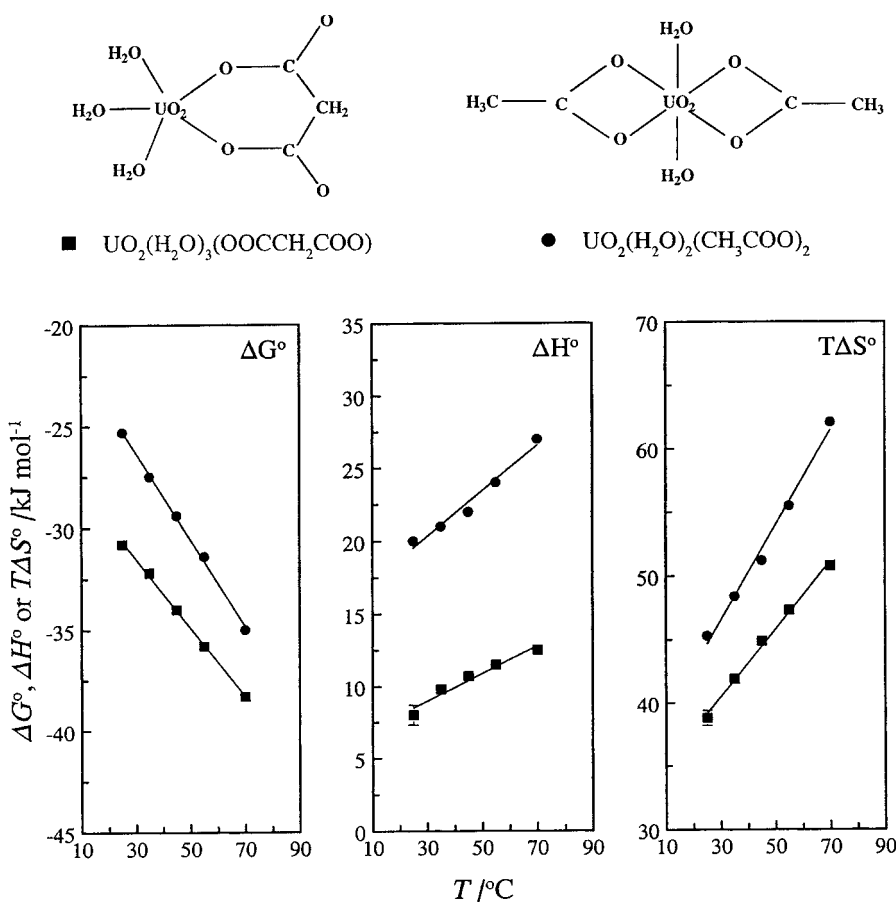


Fig. 4. Comparison of the thermodynamic parameters for the formation of $UO_2(H_2O)_3(OOCCH_2COO)$ (■), and $UO_2(H_2O)_2(CH_3COO)_2$ (●) [9].

for $\text{UO}_2(\text{OOCCH}_3)_2$. These trends could be rationalized in terms of the perturbation by the complex formation in the primary hydration sphere and the bulk water, and the degree of desolvation of the metal and ligand associated with the complexation.

For hard acid-hard base interactions, the enthalpy term largely reflects the energy required for dehydration. Reactions (6) and (7) indicate that less energy for the dehydration of the uranyl ion is required in the formation of $\text{UO}_2(\text{H}_2\text{O})_3(\text{OOCCH}_2\text{COO})$ than $\text{UO}_2(\text{H}_2\text{O})_2(\text{CH}_3\text{COO})_2$. Additionally, the dehydration of the ligands could differ between reactions (6) and (7). As shown in Fig. 4, each carboxylate group in the malonate ligand is unidentate, with one oxygen pointing toward the secondary hydration sphere or the bulk water, but all the oxygens in the acetate groups in the uranyl acetate complex are bound to uranium. This means that the malonate ligand is less dehydrated than the acetate in the complex. The difference in the dehydration of both the metal and the ligand results in the observed trend that the ΔH° for reaction (6) is larger than the ΔH° for reaction (7).

Similarly, the trend in the entropy (the $T\Delta S^\circ$ for reaction (6) is larger than the $T\Delta S^\circ$ for reaction (7)) can be interpreted based on the structural information of the uranyl acetate and malonate complexes. The cratic term ($\nu = 1$, the change of the number of species) [33] is the same for reactions (6) and (7), suggesting that the gain in the translational entropy is similar in both reactions. However, the change in the degree of disorder in the bulk solvent could be quite different. With the non-coordinating oxygens pointing outward, the uranyl malonate complex is more "hydrophilic" than the 1:2 uranyl acetate complex (Fig. 4), so that the former has a stronger structuring effect on the bulk solvent through hydrogen bonding. Consequently, the overall entropy change in reaction (7) is less than that in reaction (6). The stronger structuring effect of the malonate complex on the bulk solvent could also be responsible for the smaller temperature effect of both ΔH° and $T\Delta S^\circ$ for reaction (7), because a more ordered solvent structure is expected to be less susceptible to the thermal movements caused by higher temperature.

Acknowledgment. This work was supported by the Director, Office of Science, Office of Basic Energy Sciences, Division of Chemical Sciences, and by the Assistant Secretary for Environmental Management under U.S. Department of Energy Contract No. DE-AC03-76SF0098 at Lawrence Berkeley National Laboratory (LBNL). The EXAFS experiments were conducted at SSRL, which is operated by the Department of Energy, Division of Chemical Sciences. The authors thank the colleagues at the Glenn T. Seaborg Center of LBNL, Drs. C. W. Booth and W. W. Lukens, Jr. in particular, for the help with the EXAFS and X-ray crystallography.

References

- Cruse, J. M., Gilchrist, R. L.: Developing Waste Disposal Options in the Underground Storage Tank-Integrated Demonstration Program. In: *Global 93, Future Nuclear Systems: Emerging Fuel Cycles and Waste Disposal Options*. American Nuclear Society, La Grange Park, IL (1993) p. 1376.
- DOE, Estimating the Cold War Mortgage: The 1995 Baseline Environmental Management Report. DOE/EM-0232, U.S. Department of Energy, Washington, D.C. (1995).
- Martell, A. E., Smith, R. M.: *Critical Stability Constants*. Vol. 6, Plenum Press, New York (1989).
- Atkins, P. W.: *Physical Chemistry*. 6th Ed., W. H. Freeman, New York (1998).
- Zanonato, P., Di Bernardo, P., Bismondo, A., Rao, L., Choppin, G. R.: *J. Solution Chem.* **30**, 1 (2001).
- Helgeson, H. C., Kirkham, D. H., Flowers, G. C.: *Amer. J. Sci.* **281**, 1249 (1981).
- Tanger, J. C., Helgeson, H. C.: *Amer. J. Sci.* **288**, 19 (1988)
- Shock, E. L.: *Geochim. Cosmochim. Acta* **57**, 4899 (1993).
- Jiang, J., Rao, L., Zanonato, P., Di Bernardo, P., Bismondo, A.: *J. Chem. Soc., Dalton Trans* 1832–1838 (2002).
- Born, Von M.: *Z. Phys.* **1**, 45 (1920).
- Cassol, A., Magon, L., Tomat, G., Portanova, R.: *Inorg. Chim. Acta* **3**, 639 (1969).
- Seward, T. M.: In: *Chemistry and Geochemistry of Solutions at High Temperatures and Pressures, Physics and Chemistry of the Earth*. Vols. 13, 14 (Rickard, D. T., Wickman, F. E., eds.) Pergamon Press (1981) p. 113.
- Schwarzenbach, G.: Interpretation of solution stabilities of metal complexes, in *Proc. Summ. Sch. Stability Constants*. 1st Pub. 1977, (Paoletti, P., Barbucci, R., Fabbrizzi, L., eds.) Ed. Scient. University of Florence, Italy (1977) pp. 151–181.
- Rizkalla, E. N., Choppin, G. R.: In: *Handbook on the Physics and Chemistry of Rare Earths*. Vol. 18 – Lanthanides/Actinides: Chemistry. (Gschneider, Jr., K. A., Eyring, L., Choppin, G. R., Lander, G. H., eds.) Elsevier Science B.V., New York (1994).
- Dean, J. A.: *Analytical Chemistry Handbook*. McGraw-Hill, Inc., New York (1995) pp. 3–108.
- Sill, C. W., Peterson, H. E.: *Anal. Chem.* **19**, 646 (1947).
- Gran, G.: *Analyst* **77**, 661 (1952).
- Di Bernardo, P., Cassol, A., Tomat, G., Bismondo, A., Magon, L.: *J. Chem. Soc. Dalton* 733 (1983).
- Gans, P., Sabatini, A., Vacca, A.: *J. Chem. Soc., Dalton Trans.* 1195 (1985).
- Grenthe I., Ots, H.: *Acta Chem. Scand.* **26**, 1217 (1972).
- Sohnel, O., Novotny, P.: *Densities of Aqueous Solutions of Inorganic Substances*. Elsevier, New York (1985).
- Smith, R., Zanonato, P., Choppin, G. R.: *J. Chem. Thermodyn.* **24**, 99 (1992).
- Arnek, R.: *Arkiv Kemi* **32**, 81 (1970).
- Bucher, J. J., Edelstein, N. M., Osborne, K. P., Shuh, D. K., Madden, N., Luke, P., Pehl, D., Cork, C., Malone, D., Allen, P. G.: SRL'95 Conference Proceedings. *Rev. Sci. Instr.* **67**, 1 (1996).
- Li, G. G., Bridges, F., Booth, C. W.: *Phys. Rev. B* **52**, 6332 (1995).
- Zabinsky, S. I., Rehr, J. J., Ankudinov, A., Albers, R. C., Eller, M. J.: *Phys. Rev. B* **52**, 2995 (1995).
- Bombieri, G., Benetollo, F., Forsellini, E.: *J. Inorg. Nucl. Chem.* **42**, 1423 (1980).
- Meinrath, G., Kato, Y., Yoshida, Z.: *J. Radioanal. Nucl. Chem.* **174**, 299 (1993).
- Bell, J. T., Biggers, R. E.: *J. Mol. Spect.* **18**, 247 (1965); **22**, 262 (1967); **25**, 312 (1968).
- Wruck, D. A., Zhao, P., Palmer, C. E. A., Silva, R. J.: *J. Sol. Chem.* **26**, 267 (1997).
- Choppin, G. R., Schneider, J. K.: *J. Inorg. Nucl. Chem.* **32**, 3283 (1970).
- Archer, D. G., Wang, P.: *J. Phys. Chem. Ref. Data* **19**, 371 (1990).
- Gurney, R. W.: *Ionic Processes in Solution*. McGraw-Hill, New York (1953).
- Choppin, G. R., Unrein, P. J.: Thermodynamic Study of Actinide Fluoride Complexation. In: *Transplutonium Elements*. (Muller, W., Lindner, R., eds.) North-Holland Publishing Company, Amsterdam (1976).
- Choppin, G. R., Rao, L.: *Radiochim. Acta* **37**, 143 (1984).
- Howatson, D. M., Morosin, B.: *J. Inorg. Nucl. Chem.* **37**, 1933 (1975).
- Templeton, D. H., Zalkin, A., Ruben, H., Templeton, L. K.: *Acta Cryst. C* **41**, 1439 (1985).
- Quilès, F., Burneau, A.: *Vibrational Spectrosc.* **18**, 61 (1998).
- Denecke, M. A., Reich, T., Pompe, S., Bubner, M., Heise, K. H., Nitsche, H., Allen, P. G., Bucher, J. J., Edelstein, N. M., Shuh, D. K.: *J. Phys. IV* **7**, 637 (1997).
- Rajas, R. M., Del, P. A., Bombieri, G., Benetollo, F.: *J. Inorg. Nucl. Chem.* **41**, 541 (1979).